Journal of Ceramic Processing Research. Vol. 23, No. 6, pp. 783~793 (2022)
(Received 9 January 2022, Received in revised form 6 April 2022, Accepted 9 April 2022)
https://doi.org/10.36410/jcpr.2022.23.6.783

J O U R N A L O F
Ceramic Processing Research

Investigation and optimization on micro and nano Al_2O_3 reinforced aluminium composites using GRA coupled PCA technique

A. Srinivasan[a,*], R. Prabu[b], S. Ramesh[c] and R. Viswanathan[a]
[a]*Department of Mechanical Engineering, AVS Engineering College, Salem-636003, Tamil Nadu, India*
[b]*Department of Mechanical Engineering, Mahendra Engineering College, Namakkal -637503, Tamilnadu, India*
[c]*Department of Mechanical Engineering, Jerusalem College of Engineering, Chennai -600100, India*

Aluminum alloy are widely adopted material for engineering applications in automobile, aircraft and marine industries. Its high strength to weight ratio attracts modern industry to extend its applications in various domains. For producing various components, turning is the most reputed machining operation. The method of manufacturing directly impacts the product accuracy. The present research deals with fabrication and optimization study in dry turning of LM25 Aluminium Metal Matrix Composites (AMMCs). For AMMC fabrication, 10 wt.% of micro and nano Al_2O_3 ceramic particle is added as reinforcement. Hybrid Grey Relational Analysis (GRA) coupled Principal Component Analysis (PCA) technique is suggested for finding optimization results. Experiment was conducted with cutting speed (V), feed rate (f), and depth of cut(d) as input parameters. Based on optimization, feed rate dominates the entire turning process compared to cutting speed and depth of cut and 12.95% improvement of GRA was achieved at the end of confirmation experiment.

Key words: Al_2O_3, Ceramic composites, Hybrid optimization, LM25 alloy, Turning, GRA.

Introduction

This modern world visualized the new epoch in materials research. Specifically, development and demand of light materials is much needed in automobile industry. Aluminum alloy fulfills the needs of automobile industry due to its high strength and light weight. The present world is still in a hurry to develop different combination of lightweight materials in numerous applications [1]. Thus, the enhanced material property required in material application is fulfilled by Metal Matrix Composites (MMCs). MMCs offer enhanced material properties like minimum thermal conductivity and expansion, greater specific strength and stiffness etc. Aluminum Metal Matrix Composites (AMMCs) are widely used in huge applications due to its enriched material properties such as high strength, high fatigue etc. In aircraft and automotive sectors, AMMCs are used to reduce the parts weight, fuel and less pollution aspects [2-6].

LM25 aluminum alloy is the most widely used in automotive industry for the fabrication of cylindrical blocks, heads, wheels and other cast parts. Addition of reinforcement in AMMCs induces more strength and stiffness and offers high machinability [7-10]. Successive reinforcement characterization is noted by chemical composition, volume fraction and distribution of reinforcement particle in AMMCs [11]. Naguib G. Yakoub [12] studied the effect of nano zirconia in Al-7075 fabricated by stir casting process. He identified that ZrO_2 reduces wear rate and friction coefficient and exhibited good tribological performance. Manjunatha and Anil kumar [13] studied the mechanical characterization of aluminum Al6061/ ZrO_2/Zirconium sand hybrid composite. They stated that ZrO_2 particles in AMMCs increased the tensile strength and hardness. Addition of 10 wt.% of ZrO_2 and 2 wt.% of ZrO_2 sand induces high strength when compared with base metal. Suresh et al. [14] investigated on LM25 alloy for evaluating mechanical and wear properties. They pointed that, hardness values of LM25 alloy reinforced with B_4C (Boron Carbide) improved when compared with LM25 alloy. They also stated that, inclusion of Graphite (Gr) as reinforcement reduced the wear resistance in LM25-B_4C. At the same time, Gr in LM25-B_4C reduces hardness and material properties due to spongy nature of Gr (Graphite).

Surendaran et al. [15] examined the tribological behavior of LM25 with nano aluminum oxide (Al_2O_3). Better tribological behavior of LM25 was observed when 5 wt.% of Al_2O_3 was used amongst the other compositions selected due to even dispersion of Al_2O_3 in base metal. Elango and Raghunath [16] investigated the wear and friction resistance in LM25 alloy reinforced with Silicon Carbide (SiC) and Titanium dioxide (TiO_2). They stated that, co efficient of friction

*Corresponding author:
Tel : +91-9894852123
E-mail: srivankumar14@gmail.com

(COF) reduced with respect to raise in TiO_2. Wear rate of LM25+SiC+ 5% TiO_2 was minimum while it was compared with LM25 alloy. In material research, selection of fabrication technique, methods of machining and machining parameters are the key factors. Properties of composites are controlled by the varying reinforcement and its percentage level. Commonly selected wt.% of reinforcement is 5 wt.% while SiC, Al_2O_3 and B_4C are used as reinforcements in AMMCs. Drilling, turning and friction stir processing (FSP) are the common machining techniques adopted by researchers in AMMCs [17]. Periasamy et al. [18] analysed the mechanical properties in Al7075 by FSP technique and SiC and Gr added were selected as reinforcements. Experimental observations denote the formation of lubrication layer on the specimen due to addition of soft Gr. Significant improvement in hardness was identified in Al7075 due to the inclusion of SiC as reinforcement.

Kannan et al. [19] performed turning operation in Al7075 alloy fortified with SiC and Gr as reinforcement and found that addition of 3 wt.% SiC and 7 wt.% of Gr were identified as optimal reinforcement. Also, they pointed that parameters of 40 m/min cutting speed, 0.075 mm/rev feed and 0.3 mm depth of cut offered dominant impact on surface roughness of turned AMMCs and tool wear. At optimum condition, surface roughness improved by 16% and tool wear reduced by 22%. Hence performing optimization is much needed in material machining research. Optimization in machining parameters results in high precision outputs. Numerous research works were carried out in optimization techniques in which ANOVA, GRG (Grey Relational Grade) and GRC (Grey Relational Coefficient) are the most familiar techniques [20]. TOPSIS technique is also used in machining parameter optimization. In material turning and optimization, machining parameters such as feed, depth and cutting parameters played a key factor [21-24]. Dhanalakshmi and Rameshbabu [25] performed an investigation about influencing parameter on LM25 under dry condition. They reported about obtaining high GRG value in wet machining. Based on the experiments, 500 rpm cutting speed, 0.2 mm/min feed and 0.6 mm depth of cut were the optimum parameters while machining in CNC Machine.

On reviewing the past study, numerous researches were performed on AMMCs under various circumstances. Lot of research is carried out in improving materials. Based on past examination, it is evident that selection of reinforcement was done in the base of wt.% only. Hence influence of reinforcement size on machining need to be investigated. This paper is forced on optimization of machining parameters and size of reinforcement. For the present research, LM25 Al was selected and Al_2O_3 was chosen as reinforcement.

Materials and Methods

AMMCs were fabricated by stir casting process with 10 wt.% of micro and nano Al_2O_3 particles as reinforcement. The average particle size of micro and nano alumina is 25 μm and 40 nm respectively. Initially a base metal is melted using electrical induction heating furnace in a graphite crucible at 720 °C. The mixing of Al_2O_3 particles along with base metal is done by mechanical stirring mode at 650 rpm. Lastly, it is poured into a zircon coated steel die. The hardness of the fabricated composite specimen was found as 36 HRB and 58 HRB for micro and nano Al_2O_3 reinforced composites respectively. Fig. 1 shows the experimental setup. Fig. 2 and 3 represents the SEM image of micro and nano Al_2O_3 particles reinforced AMMCs at different magnifications and it is

Table 1. Machining factors with levels.

Symbol	Control factors	Level 1	Level 2	Level 3
A	Alumina size	Micro Al_2O_3	Nano Al_2O_3	
V	Cutting speed (m/min)	100	125	150
f	Feed (mm/rev)	0.1	0.15	0.2
d	Depth of cut(mm)	0.5	0.75	1.0

Fig. 1. (a) Experimental setup. (b) Stir casting setup.

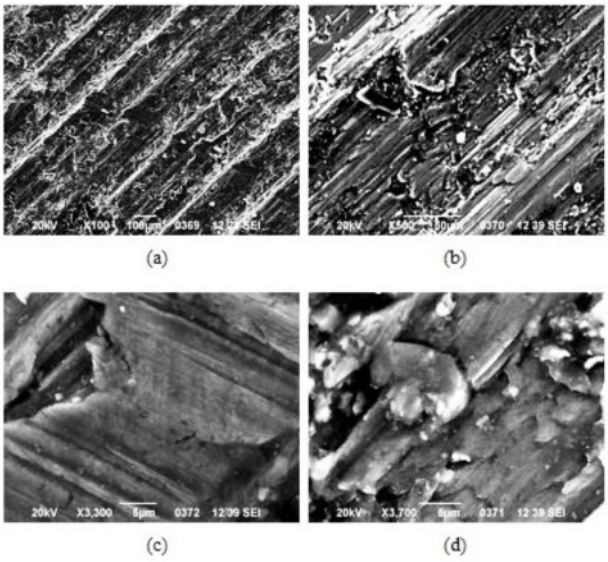

Fig. 2. SEM image of micro Al_2O_3 reinforced composites (a) 100×; (b) 500×; (c) 3300× and (d) 3700×.

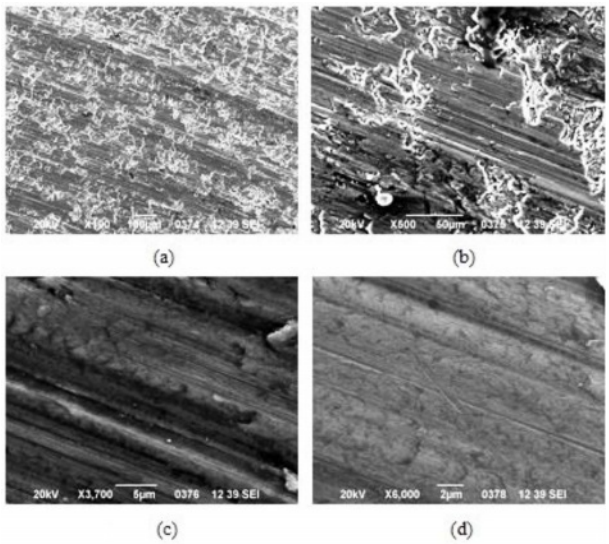

Fig. 3. Fig. 5 SEM images of nano Al_2O_3 reinforced composites: (a) 100×; (b) 500×; (c) 3700× and (d) 6000×.

observed that no pores have been observed and indicate better wettability between the matrix and reinforcement particles. This research focused on performing turning operation in LM25 Al MMC under dry condition. Kirloskar Turn Master all geared type lathe machine is used to perform turning operation. Selected parameters for performing turning operation are based on earlier findings [19, 26-29] and given in Table 1. For optimization, L18 orthogonal array was selected. Surface roughness (Ra), cutting force (Fz), tool wear (V_B) and tool temperature (T) were the output parameters which are measured by TR100 surface roughness tester, Kistler dynamometer (SN type), tool maker's microscope and tool temperature thermocouple setup respectively as shown in Fig. 4. Calculated experimental values are represented in Table 2.

Table 2. Calculated experimental values.

S. No	A	'V' (m/min)	'f' (mm/rev)	'd' (mm)	'V_B' (mm)	'Ra' (μm)	'Fz' (N)	'T' (°C)
1	1	100	0.1	0.5	0.10	1.32	60.55	44
2	1	100	0.15	0.75	0.08	1.34	153.66	57
3	1	100	0.2	1.0	0.1	1.62	262.06	57
4	1	125	0.1	0.5	0.06	0.99	37.91	45
5	1	125	0.15	0.75	0.09	1.08	68.23	55
6	1	125	0.2	1.0	0.17	1.32	257.14	75
7	1	150	0.1	0.75	0.08	0.97	42.15	56
8	1	150	0.15	1.0	0.13	1.25	52.78	62
9	1	150	0.2	0.5	0.15	1.37	56.86	68
10	2	100	0.1	1.0	0.09	1.28	152.3	43
11	2	100	0.15	0.5	0.06	1.42	87.29	48
12	2	100	0.2	0.75	0.90	1.17	238.76	57
13	2	125	0.1	0.75	0.06	0.97	146.65	52
14	2	125	0.15	1.0	0.10	1.39	120.57	58
15	2	125	0.2	0.5	0.13	2.36	101.2	60
16	2	150	0.1	1.0	0.14	1.09	123.56	68
17	2	150	0.15	0.5	0.38	1.34	156.78	72
18	2	150	0.2	0.75	0.57	1.67	187.45	78

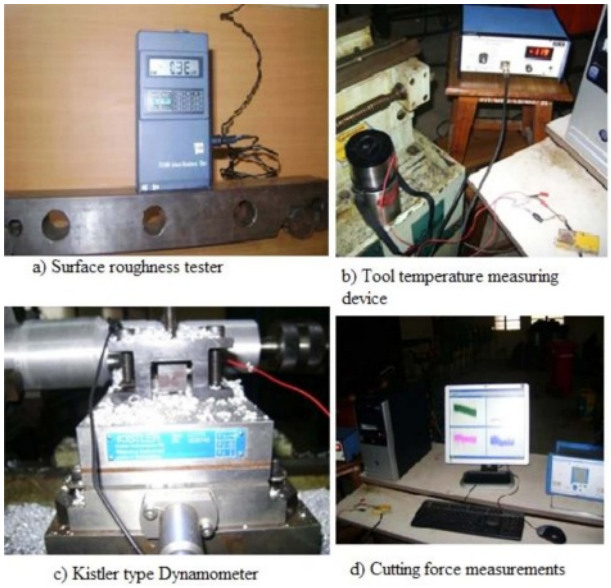

Fig. 4. Measurement of responses.

GRA Combined Through PCA Technique

Grey Relational Analysis (GRA)

GRA is used to find the optimal machining parameters and cutting conditions while using multi response complex problems [30, 31]. Rank system is used to find the best optimal values. The following effective steps are used for finding GRC and GRG.

STEP 1: Calculation of S/N ratio is the first step of GRA. This article concentrated on minimizing the response for optimal conditions.

$$S/N = -10\log\frac{1}{n}\left(\sum_{i=1}^{n} y_i^2\right) \tag{1}$$

N = No. of observations and y = observed data.

STEP 2: Normalization is the second stage in GRA technique. The response value obtained from S/N ratio normalized is by normalization formula. Suitable formula for obtaining the normalized value is represented in eq. (2).

$$x_i(k) = \frac{\max\left|x_i^0(k)\right| - x_i^0(k)}{\max\left|x_i^0(k)\right| - \min\left|x_i^0(k)\right|} \tag{2}$$

$x_i(k)$ = Value of normalization, k = performance characteristics, i = no. of experiments

STEP 3: The expression used to compute GRC value is given below.

$$\varepsilon(k) = \frac{\min_j \min_k \left|x_0(k) - x_j(k)\right| + \xi \max_j \max_k \left|x_0(k) - x_j(k)\right|}{\left|x_0(k) - x_j(k)\right| + \xi \max_j \max_k \left|x_0(k) - x_j(k)\right|} \tag{3}$$

Here, ε(k)= grey relational coefficient

j = 1, 2, 3… n
k = 1, 2, 3…. m
n = experimental data
m = observed performance characteristic.
Distinguishing coefficient (ξ) = 0.5.

STEP 4: Average value of GRC is used to find the GRG value. The expression used to determine the GRG is presented in Eq. (4).

$$\gamma_i = \frac{1}{n}\sum_{k=1}^{n} \varepsilon_i(k) \tag{4}$$

Where k = performance characteristics, i = no. of experiments

Principal component analysis (PCA)

The current work is focused on performance characteristics and finding suitable input parameters. Shihab et al. [32] carried an investigation and studied about GRA and PCA in turning of alloy steel and found both GRA and PCA to be effective methods of optimization. Following steps are adopted for PCA technique [33].

STEP 1: In PCA, normalization of output performance is considered as first step. Here x_i^k is considered as output responses. The normalization value of output performance is calculated by Eq. (5) and (6).

$$X_i^k = \frac{\min x_i^k}{x_i^k} \tag{5}$$

$$X_i^k = \frac{x_i^k}{\max x_i^k} \tag{6}$$

Where k = 1, 2, 3…n

n = no. of output characteristics
i = 1, 2, 3…m
m = no. of Experiments

STEP 2: The second step of PCA technique indicates the determination of covariance matrix, Eigen values and Eigen vectors. The covariance matrix is expressed in Eq. (7)

$$Covariance\ Matrix\ M = \begin{matrix} M11 & \dots & M1n \\ \vdots & \dots & \vdots \\ Mm1 & \dots & Mmn \end{matrix} \tag{7}$$

The Eigen values are denoted by λ_k. It is calculated by Eq. (8).

$$\left(M - \lambda_k \mathrm{I_m}\right) V_{ik} = 0 \tag{8}$$

Where V_{ik} = Corresponding Eigen Vectors
M= Covariance matrix.

STEP 3: The final step of PCA indicates the individual principal component formation and it is expressed in Eq. (9)

$$Y_{mk} = \Sigma_i^n Y_{ik} V_{ik} \quad (9)$$

Results and Discussion

The main aim of this experimental work is to diminish the V_B, Ra, F_Z and T. Based on Eq. (1), S/N ratio of output responses was calculated and plotted in Table 3.

GRG Analysis

The normalization values of measured output values were determined by using Eq. (2) and normalized values are plotted in Table 4. The corresponding GRC values were determined by using Eq. (3) and it is represented in Table 5. In this work, GRA and PCA are coupled with each other to evaluate the optimal cutting conditions. Later, PCA is used to determine the influencing parameters among all values. The correlation coefficient amount targeted quality characters are calculated and presented in Table 6 and its performance features are given in Table 7. The Eigen vectors of each performance feature are plotted in Table 8. Performance characteristics of principal components are determined by adding Eigen vectors and it is given in Table 9. Based on plotted Table 7, principal component one features high as 57.87% compared to remaining three principal components. After calculation of weighted values, GRG values were found by using Eq. (4). The ranks of parameters with GRG values are presented in Table 10. Based on GRG, maximum GRG represents best quality characteristics.

Table 3. S/N ratio of response.

Expt. No.	V_B	R_a	F_Z	T
1.	20.000	-2.411	-35.642	-32.869
2.	21.938	-2.542	-43.731	-35.117
3.	20.000	-4.190	-48.368	-35.117
4.	24.437	0.087	-31.575	-33.064
5.	20.915	-0.668	-36.680	-34.807
6.	15.391	-2.411	-48.203	-37.501
7.	21.938	0.265	-32.496	-34.964
8.	17.721	-1.938	-34.449	-35.848
9.	16.478	-2.734	-35.096	-36.650
10.	20.915	-2.144	-43.654	-32.669
11.	24.437	-3.046	-38.819	-33.625
12.	0.915	-1.364	-47.559	-35.117
13.	24.437	0.265	-43.326	-34.320
14.	20.000	-2.860	-41.625	-35.269
15.	17.721	-7.458	-40.104	-35.563
16.	17.077	-0.749	-41.838	-36.650
17.	8.404	-2.542	-43.906	-37.147
18.	4.883	-4.454	-45.458	-37.842

Table 4. Normalization value.

Expt. No.	V_B	Ra	F_Z	T
1.	0.952	0.748	0.899	0.971
2.	0.976	0.734	0.484	0.600
3.	0.952	0.532	0.000	0.600
4.	1.000	0.986	1.000	0.943
5.	0.964	0.921	0.865	0.657
6.	0.869	0.748	0.022	0.086
7.	0.976	1.000	0.981	0.629
8.	0.917	0.799	0.934	0.457
9.	0.893	0.712	0.915	0.286
10.	0.964	0.777	0.490	1.000
11.	1.000	0.676	0.780	0.857
12.	0.000	0.856	0.104	0.600
13.	1.000	1.000	0.515	0.743
14.	0.952	0.698	0.631	0.571
15.	0.917	0.000	0.718	0.514
16.	0.905	0.914	0.618	0.286
17.	0.619	0.734	0.470	0.171
18.	0.393	0.496	0.333	0.000

Table 5. Computed GRC value.

Expt. No.	V_B	Ra	F_Z	T
1.	0.913	0.665	0.832	0.946
2.	0.955	0.653	0.492	0.556
3.	0.913	0.517	0.333	0.556
4.	1.000	0.972	1.000	0.897
5.	0.933	0.863	0.787	0.593
6.	0.792	0.665	0.338	0.354
7.	0.955	1.000	0.964	0.574
8.	0.857	0.713	0.883	0.479
9.	0.824	0.635	0.855	0.412
10.	0.933	0.692	0.495	1.000
11.	1.000	0.607	0.694	0.778
12.	0.333	0.777	0.358	0.556
13.	1.000	1.000	0.508	0.660
14.	0.913	0.623	0.576	0.538
15.	0.857	0.333	0.639	0.507
16.	0.840	0.853	0.567	0.412
17.	0.568	0.653	0.485	0.376
18.	0.452	0.498	0.428	0.333

Table 6. Correlation coefficients.

Correlation coefficients	V_B	R_a	F_Z	T
V_B	1	0.4049	0.4228	0.7000
R_a	0.4049	1	0.4370	0.2883
F_Z	0.4228	0.4370	1	0.3483
MRR	0.7000	0.2883	0.3483	1

Table 7. Computed Eigen value.

Principal component	λ_k	Explained variation (%)
PC1	2.3147	57.87
PC2	0.8374	20.94
PC3	0.5609	14.02
PC4	0.2869	7.17

Table 8. Computed Eigen vectors.

Response	PC1	PC2	PC3	PC4
V_B	0.5629	0.3515	0.095	0.742
R_a	0.4423	-0.604	0.6497	-0.1327
F_Z	0.4658	-0.4616	-0.754	-0.0382
MRR	0.5201	0.5465	0.02	-0.6561

Table 9. Contribution value for the PCs.

PC	Contribution
V_B	0.317
R_a	0.196
F_Z	0.217
MRR	0.271

Table 10. Rank based on GRG.

Expt. No.	GRG	Rank
1.	0.857	3
2.	0.688	9
3.	0.614	13
4.	0.968	1
5.	0.797	7
6.	0.551	15
7.	0.863	2
8.	0.733	8
9.	0.683	10
10.	0.810	4
11.	0.797	6
12.	0.486	17
13.	0.802	5
14.	0.682	11
15.	0.613	14
16.	0.668	12
17.	0.515	16
18.	0.424	18

Table 11. GRG Response table.

Machining Parameters	Level 1	Level 2	Level 3	Max-Min	Rank
A	0.7502	0.6443	-	0.1060	2
V	0.7086	0.7355	0.6477	0.0878	3
f	0.8279	0.7021	0.5617	0.2662	1
d	0.7388	0.6767	0.6763	0.0625	4

*Optimal Parameters = $A_1V_2f_1d_1$

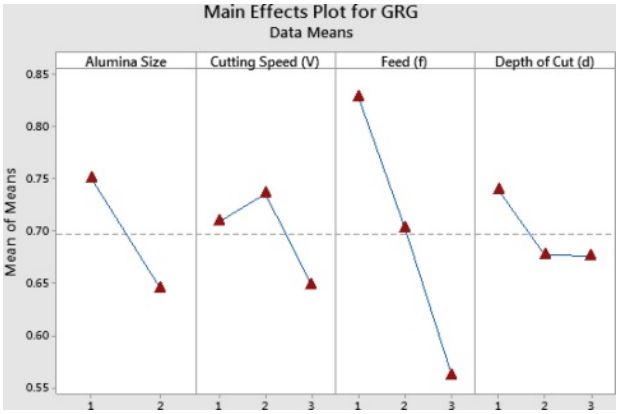

Fig. 5. Mean response plot for GRG.

Maximum GRG value was obtained in experiment four. Among 27 experiments, the maximum GRG of 0.968 was achieved. The optimum parameter for machining LM25 is evaluated from GRG and it is plotted in Table 11. From Table 11, $A_1V_2f_1d_1$ is indicated as optimum condition for dry turning of AMMCs. Micro Al_2O_3 is preferred when compared to nano reinforcement. Likewise, 125 m/min cutting speed, 0.1 mm/rev feed and 0.5 mm depth of cut were identified as optimum parameters and represented in Fig. 5. Based on analysis of variance technique, identification of dominant factor is much easier [34-36]. From Table 11, it is evident that feed rate is the most dominant factor followed by alumina size and cutting speed.

By utilizing the optimal parameters, confirmation

Table 12. Confirmation test.

	Initial parameters	Optimal Parameters	
		Prediction	Experiment
Setting level	$A_1V_1f_1d_1$	$A_1V_2f_1d_1$	$A_1V_2f_1d_1$
VB (mm)	0.10	--	0.06
Ra (μm)	1.32	--	0.99
F (N)	60.55	--	37.91
T (°C)	44	--	45
GRG	0.857	0.961	0.968
Improvement in GRG = **0.111**			

experiment was carried out to examine the accuracy of the optimization result [37]. Table 12 indicates the confirmation test. Improvement in GRG was registered by 12.95% when compared with initial experiment.

Analysis of variance

ANOVA study was computed to identify the most influencing factor on each parameter. Response surface methodology (RSM) is a key factor for researchers

Table 13. ANOVA - V_B.

Source	DF	Adj SS	Adj MS	F-Value	P-Value
Model	13	0.652908	0.050224	1.24	0.459
Linear	4	0.347981	0.086995	2.14	0.240
A	1	0.186462	0.186462	4.59	0.099
V	1	0.020425	0.020425	0.50	0.517
f	1	0.181475	0.181475	4.47	0.102
d	1	0.000395	0.000395	0.01	0.926
Square	3	0.152920	0.050973	1.25	0.402
V×V	1	0.102066	0.102066	2.51	0.188
f×f	1	0.002660	0.002660	0.07	0.811
d×d	1	0.052465	0.052465	1.29	0.319
2-Way Interaction	6	0.150525	0.025087	0.62	0.716
A×V	1	0.014908	0.014908	0.37	0.577
A×f	1	0.019203	0.019203	0.47	0.530
A×d	1	0.037921	0.037921	0.93	0.389
V×f	1	0.006879	0.006879	0.17	0.702
V×d	1	0.001523	0.001523	0.04	0.856
f×d	1	0.066531	0.066531	1.64	0.270
Error	4	0.162542	0.040635		
Total	17	0.815450			

R^2=90.07%

Table 14. ANOVA - Ra.

Source	DF	Adj SS	Adj MS	F-Value	P-Value
Model	13	1.66971	0.128439	3.83	0.102
Linear	4	0.34733	0.086833	2.59	0.189
A	1	0.01064	0.010638	0.32	0.603
V	1	0.14296	0.142962	4.27	0.108
f	1	0.13960	0.139602	4.17	0.111
d	1	0.02528	0.025276	0.75	0.434
Square	3	0.34456	0.114855	3.43	0.132
V×V	1	0.04863	0.048630	1.45	0.295
f×f	1	0.05863	0.058635	1.75	0.256
d×d	1	0.24125	0.241255	7.20	0.055
2-Way Interaction	6	0.61817	0.103029	3.08	0.148
A×V	1	0.24780	0.247803	7.40	0.053
A×f	1	0.24216	0.242164	7.23	0.055
A×d	1	0.21534	0.215344	6.43	0.064
V×f	1	0.07721	0.077206	2.30	0.204
V×d	1	0.00173	0.001727	0.05	0.831
f×d	1	0.35613	0.356128	10.63	0.031
Error	4	0.13398	0.033495		
Total	17	1.80369			

R^2=92.57%

aimed at developing quadratic model. For output response and arithmetic model development, RSM was utilized [38, 39]. To get better optimization results, V_B, R_a, F_z and T empirical model was developed and expressed in Eq. (10) to Eq. (13).

$$V_B = 3.47 - 0.177\ A - 0.0537\ V - 8.7\ f + 0.68\ d + 0.000265\ V\times V + 11.3\ f\times f - 2.00\ d\times d - 0.00313\ A$$

Table 15. ANOVA - Fz.

Source	DF	Adj SS	Adj MS	F-Value	P-Value
Model	13	84493.3	6499.5	5.04	0.065
Linear	4	35284.5	8821.1	6.84	0.045
A	1	10993.4	10993.4	8.52	0.043
V	1	3099.6	3099.6	2.40	0.196
f	1	8818.4	8818.4	6.84	0.059
d	1	5276.7	5276.7	4.09	0.113
Square	3	7006.7	2335.6	1.81	0.285
V×V	1	1386.9	1386.9	1.07	0.358
f×f	1	3544.1	3544.1	2.75	0.173
d×d	1	2183.5	2183.5	1.69	0.263
2-Way Interaction	6	21078.4	3513.1	2.72	0.176
A×V	1	2517.9	2517.9	1.95	0.235
A×f	1	2371.7	2371.7	1.84	0.247
A×d	1	574.1	574.1	0.44	0.541
V×f	1	230.5	230.5	0.18	0.694
V×d	1	2060.2	2060.2	1.60	0.275
f×d	1	5294.0	5294.0	4.10	0.113
Error	4	5160.6	1290.2		
Total	17	89653.9			

R^2=94.24%

Table 16. ANOVA - T.

Source	DF	Adj SS	Adj MS	F-Value	P-Value
Model	13	1703.14	131.011	3.82	0.103
Linear	4	1113.45	278.362	8.12	0.033
A	1	24.22	24.222	0.71	0.448
V	1	715.10	715.103	20.86	0.010
f	1	397.10	397.105	11.58	0.027
d	1	9.24	9.241	0.27	0.631
Square	3	30.01	10.004	0.29	0.830
V×V	1	15.82	15.825	0.46	0.534
f×f	1	0.36	0.364	0.01	0.923
d×d	1	14.79	14.787	0.43	0.547
2-Way Interaction	6	185.75	30.958	0.90	0.567
A×V	1	93.85	93.853	2.74	0.173
A×f	1	30.75	30.750	0.90	0.397
A×d	1	0.16	0.156	0.00	0.949
V×f	1	1.39	1.392	0.04	0.850
V×d	1	10.09	10.087	0.29	0.616
f×d	1	8.21	8.214	0.24	0.650
Error	4	137.14	34.285		
Total	17	1840.28			

R^2=92.55%

×V + 2.29 A×f + 0.644 A×d - 0.0277 V×f
- 0.0026 V×d + 11.45 f×d (10)

(Ra= 2.98 - 1.726 A + 0.0100 V - 17.0 f + 0.42 d
- 0.000183 V×V + 52.9 f×f + 4.30 d×d+ 0.01275 A×V
+ 8.13 A×f - 1.534 A×d + 0.0928 V×f - 0.0028 V×d
- 26.48 f×d (11)

Fz = 418 + 82 A - 7.34 V - 3779 f + 736 d + 0.0309 V
×V + 13018 f×f - 409 d×d + 1.286 A×V - 805 A×f
- 79 A×d - 5.1 V×f - 3.03 V×d + 3229 f×d (12)

T= 87 - 13.3 A - 1.07 V + 103 f + 11 d + 0.00330 V×V
+ 132 f×f - 33.6 d×d + 0.248 A×V - 91.7 A×f
- 1.3 A×d + 0.39 V×f + 0.212 V×d + 127 f×d (13)

The computed value of ANOVA for V_B, Ra, Fz and T are given in Table 13, 14, 15 and 16 respectively. From table values, it is evident that the R^2 value of V_B, Ra, Fz and T are 90.07, 92.57, 94.24 and 92.55% respectively. Hence based on R^2 value represents the significant model development [40-42].

Mean response plot for all the parameters was drawn for further analysis. Fig. 6 to Fig. 9 represents the main effect plot for V_B, Ra, Fz and T respectively. To minimize tool wear, parameters such V=150 m/min, f=0.2 mm/rev, d=0.75 mm and nano size reinforcement

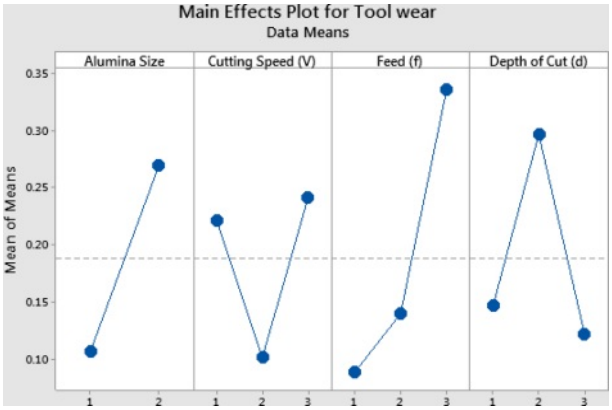

Fig. 6. Mean response plot- V_B.

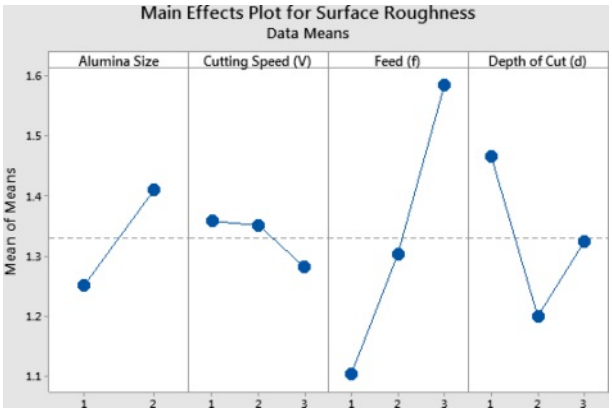

Fig. 7. Mean response plot- Ra.

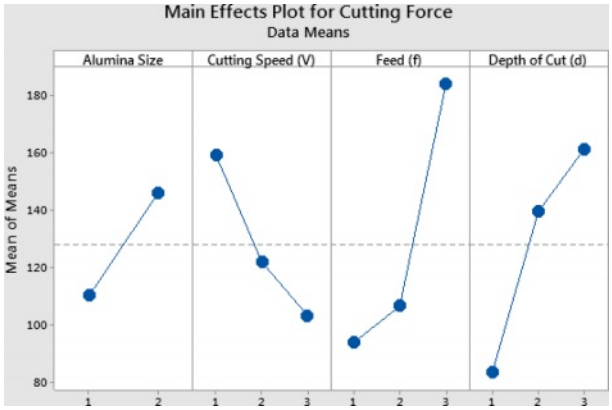

Fig. 8. Mean response plot - F_z.

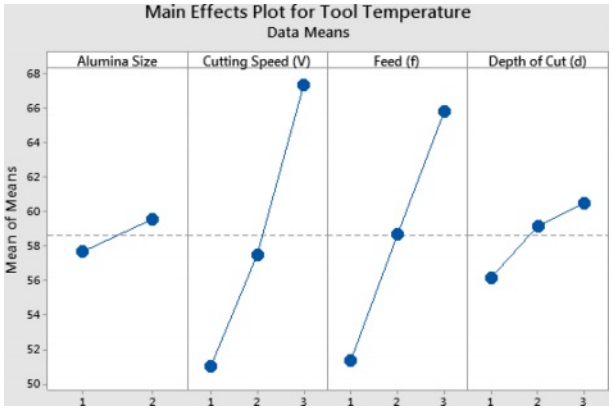

Fig. 9. Mean response plot- T.

are suitable factors. For all the output response, nano Al_2O_3 is preferred. Nano reinforcement offered uniform distribution of the particles. High depth of cut results in higher wear. So, moderate depth would reduce the tool wear. Reinforcement like hard alumina increases the hardness of the AMMCs. Hence, nano reinforcement offered good strength to the MMCs and does not affect the tool.

For roughness, V=100 m/min, f=0.15 mm/rev, d=0.5 mm and nano size reinforcement are the optimum parameters. For cutting force, V=100 m/min, f=0.20 mm/rev, d=1 mm and Nano size reinforcement are the optimum parameters and for temperature, V=150 m/min, f=0.20 mm/rev, d=1 mm and Nano size reinforcement are the optimum parameters. Table 17 represents the responses of V_B, Ra & Fz. It is evident that for V_B, feed is the dominant factor compared with cutting speed and depth of cut. At the same time, for Ra, cutting speed is the most dominant factor. It dominates 50.25% when compared with other parameters. For Fz, cutting speed dominated at 32%. At high cutting speed, temperature raise could affect the tool and surface [25]. Similarly for T, cutting speed was found as dominant factor with 51.29%. These are in line with similar findings made by Kannan [19].

Table 17. ANOVA for responses V_B, Ra & Fz.

a) For V_B					
Source of variance	DF	Adj SS	Adj MS	F -Value	PC (%)
A	1	0.12005	0.12005	3.83	22.49
V	2	0.0688	0.03440	1.10	12.89
f	2	0.20603	0.10302	3.29	38.61
d	2	0.1075	0.05375	1.72	20.14
Error	10	0.031307	0.003131		5.87
Total	17	0.533687			100.00
b) For Ra					
Source of variance	DF	Adj SS	Adj MS	F -Value	PC (%)
A	1	0.11361	0.11361	1.51	8.12
V	2	0.21640	0.10820	1.14	15.47
f	2	0.70268	0.35134	4.67	50.25
d	2	0.21361	0.10681	1.42	15.27
Error	10	0.15216	0.01522		10.88
Total	17	1.39846			100.00
c) For Fz					
Source of variance	DF	Adj SS	Adj MS	F -Value	PC (%)
A	1	26239	26239	4.56	29.27
V	2	28513	14256	5.43	31.80
f	2	9695	4848	1.85	10.81
d	2	19403	9702	3.70	21.64
Error	10	5804	580		6.47
Total	17	89654	26239		100.00
d) For T					
Source of variance	DF	Adj SS	Adj MS	F -Value	PC (%)
A	1	16.06	16.06	0.50	1.02
V	2	811.44	405.72	12.57	51.29
f	2	630.78	315.39	9.77	39.87
d	2	59.11	29.56	0.92	3.74
Error	10	64.58	32.29		4.08
Total	17	1581.97			100.00

Conclusion

Based on LM25 AMMCs turning, the following conclusions are made and listed below.

1. To determine the dominating parameter in dry turning of LM25 AMMCs, GRA coupled PCA optimization technique was suggested and feed rate was found as dominating parameter.

2. The optimal parameter based on GRA coupled PCA technique are 125 m/min cutting speed, 0.1 mm/rev feed and 0.5 mm depth of cut. For better reinforcement composition, micro Al_2O_3 is preferred when compared with nano reinforcement.

3. Based on ANOVA analysis, the influencing factor of each parameter was found i.e., feed is the dominant factor V_B and cutting speed for Ra, Fz and T respectively.

4. RSM analysis represents effectiveness of the regression model. Based on RSM, it was found that, R^2 value of V_B, Ra, Fz and T are 90.07, 92.57, 94.24 and 92.55% respectively. It represents significant model development.

5. After conducting confirmation experiment, improvement in GRG was registered by 12.95% when compared with initial experiment.

References

1. P.K. Jain, S.C. Soni and P.V. Baredar, Mater. Sci. Res. India. 11[2] (2014) 114-120.
2. I. Mohammed and A.R. Anwar Khan, J. Mater. Res. Technol. 8[3] (2019) 3347-3356.
3. P. Rambabu, N. Eswara Prasad, V.V. Kutumbarao and R.J.H. Wanhill. Ind. Inst. Met. Series (2017) 29-51.
4. D.S. Prasad, C. Shoba and N. Ramanaiah, J. Mater. Res. Technol. 3 (2014) 79-85.
5. J. Umar Mohamed, P.L.K. Palaniappan, P. Maran and R. Pandiyarajan, J. Ceram. Process. Res. 22[3] (2021) 306-316.
6. A. Elaya Perumal, G.R. Jinu, S. Vidhyalakshmi and S. Amal Bosco Jude, J. Ceram. Process. Res. 21[5] (2020) 524-532.
7. T.R. Sorena, K. Ramanuj, I. Panigrahia, A.K. Sahooa, A. Pandaa and R.K. Dasa, Mater. Today Proc. 18 (2019) 50 69-75.
8. L. Krishnamurthy and B.K. Sridhara, Int. J. Mach. Mach. Mater. 10[12] (2011) 137-152.
9. M. Thirumal Azhagan and B. Mohan, J. Ceram. Process. Res. 22[4] (2021) 470-474.
10. T. Tamilanban, T.S. Ravikumar, C. Gopinath and S. Senthilrajan, J. Ceram. Process. Res. 22[6] (2021) 629-635
11. P. Narayanasamy, N. Selvakumar and P. Balasundar, Comp. Trans. Ind. Inst. Met. 68[5] (2015) 911-925.
12. N.G. Yakoub, Int. J. Sci. Technol. Res. 9[8] (2020) 417-421.
13. B.R. Manjunatha and A. Anil kumar, Int. J. Eng. Res. Tech. 4[31] (2016) 1-5.
14. V. Suresh, P. Vikram, R. Palanivel and R.F. Laubscher, Mat. Today Proc. 5 (2018) 27852-27860.
15. R. Surendran, A. Kumaravel and S. Vignesh, IOSR J. Mech. Civ. Eng. 11[3] 1-7.
16. G. Elango and B.K. Raghunath, Proc. Eng. 64 (2013) 671-680.
17. S.K. Lalmuan, S. Das, M. Chandrasekarana, and S.K. Tamang, Mat. Today Proc. 4 (2017) 8167-8175.
18. K. Periasamy, N. Sivashankar, S. Chandrakmar and R. Viswanathan, Int. J. Innov. Technol. Explor. Eng. 9 (2020) 278-281.
19. A. Kannan, R. Mohan, R. Viswanathan and N. Sivashankar, J. Mat. Res. Tech. 9[6] (2020) 16529-16540.
20. N. Sivashankar, R. Viswanathan and K. Periasamy, Mat. Today Proc. 37[2] 2020 214-219.
21. R. Viswanathan, S. Ramesh, S. Maniraj and V. Subburam, Measurement 159 (2020).
22. S. Ramesh, R. Viswanathan and S. Ambika S. Measurement 78 (2015) 63-72.
23. R. Viswanathan, S. Ramesh and V. Subburam, Measurement

120 (2018) 107-113.
24. S. Sakthivelu, T. Anandaraj and M. Selwin, Mech. Mech. Eng. 21[1] (2017) 95-103.
25. S. Dhanalakshmi and T. Rameshbabu, Mat. Today: Proc. 39[1] (2021) 48-53.
26. P. Suresh and P. Mathiyalagan, J. Mat. Sci. Mech. Eng. 3[3] (2016) 192-196.
27. A. Srinivasan, R.M. Arunachalam, S. Ramesh and J.S. Senthilkumaar, American J. App. Sci. 9[4] (2012) 478-483.
28. X. Li and WKH Seah, Wear 247 (2001) 161-171.
29. S.S. Joshi and D.M. Pendse, Mach. Sci.Technol. 8[1] (2004) 85-102.
30. J. Deng, J. Grey Sys. 1[1] (1989) 1-24.
31. L.K. Pan, C.C. Wang, S.L. Wei and H.F. Sher, J. Mat. Proc. Tech. 182 (2007) 107-116.
32. S.K. Shihab, Z.A. Khan and A.N. Siddiquee, Int. J. Eng. Trends Technol. 38[5] (2016) 238-245.
33. N. Kaushik and S. Singhal, Prod. Manuf. Res. 6[1] (2018) 171-189.
34. A. Gok, Measurement 70 (2015) 100-109.
35. A. Gok, C. Gologlu and H.I. Demirci, Int. J. Adv. Manuf. Technol. 69 (2013) 1063-1078.
36. A. Gok, K. Gok, M.B. Bilgin and M.A. Alkan, Mater. Technol. 51[6] (2017) 957-965.
37. M. Srinivasan, S. Ramesh, S. Sundaram and R. Viswanathan, J. Ceram. Process. Res. 22[3] (2021) 345-355.
38. D.I. Lalwani, N.K. Mehta and P.K. Jain, J. Mater. Process. Technol. 206 (2008) 167-179.
39. P.D. Selvaraj, P. Chandramohan and M. Mohanraj, Measurement 49 (2014) 205-215.
40. T. Pridhar, K. Ravikumar, B. Sureshbabu, R. Srinivasan, and B. Sathishkumar, Int. J. Ceram. Process. Res. 21[2] (2020) 131-142.
41. R. Srinivasan, B. Suresh Babu, P. Prathap, Ruban Whenish, R. Soundararajan and G. Chandramohan, Int. J. Ceram. Process. Res. 22[1] (2021) 16-24.
42. P. Muthurasu and M. Kathiresan, Int. J. Ceram. Process. Res. 22[6] (2021) 697-704.